Radial Distortion in Silicon Lens-Integrated THz Cameras

Robin Zatta, Ullrich R. Pfeiffer

2021 46th International Conference on Infrared, Millimeter, and Terahertz Waves (IRMMW-THz) at https://doi.org/10.1109/IRMMW-THz50926.2021.9567497

Radial Distortion in Silicon Lens-Integrated THz Cameras

Robin Zatta and Ullrich R. Pfeiffer *Fellow, IEEE*
Institute for High-Frequency and Communication Technology, University of Wuppertal, Germany
Email: zatta@uni-wuppertal.de

***Abstract*—Silicon lenses are widely employed to turn a terahertz (THz) focal-plane array into a THz camera. For the first time, we have identified the type of radial distortion caused by such lenses. To this end, we measured all single-pixel far-field radiation patterns of a 15-mm diameter 2.75-mm extended hemispherical silicon lens-integrated 32×32-pixel CMOS camera at 0.652 THz. From this, a beam incidence angle grid has been generated, indicating barrel distortion. The measured beam incidence angle is compared to a previously published closed-form relation between scan angle and feed position for extended hemispherical lenses. The presented results are essential for all beam switching applications based on dielectric extended hemispherical lenses with an elliptical extension realized in the lens center.**

I. Introduction

SILICON lenses are one solution to project the 2-D imaging aperture of a terahertz (THz) focal-plane array (FPA) on an angular field-of-view (FoV) and to equip the FPA with an angular resolution [1], [2]. In other words, they transform a THz FPA imager into a THz camera. However, because of the physics of light, every lens produces non-perfect, distorted images. This distortion should not be confused with spherical aberrations, causing blurring toward image edges. In contrast, lens distortion is the deviation from rectilinear projection, in which straight lines of a scene remain straight in an image, usually classified into three types: *radial distortion*, *decentering distortion*, and *thin prism distortion*. For most lenses, radial distortion defines the predominant component. The two main types of radial distortion are *barrel distortion* and *pincushion distortion*. In barrel distortion, image magnification decreases with distance from the optical axis. More specifically, straight lines are curved inward in the shape of a barrel. The opposite applies to pincushion distortion. Here, straight lines are curved outward in the shape of a pincushion. Mostly, both such radial distortion types are highly undesirable in imaging, but nevertheless, they can be easily fixed in post-processing, if known. Radial distortion caused by silicon lenses has not yet been researched. Here, we present first insights into the radial distortion of such lenses, based on investigations of a silicon lens-integrated 32×32-pixel CMOS THz camera [2].

II. Experiment and Results

Single-pixel far-field radiation patterns were measured for all 1024 camera pixels to identify their 2-D beam incidence angle coordinate, allowing to render a beam incidence angle grid. From this grid, the type of lens distortion can then be observed. To this end, the experimental setup, as shown in Fig. 1, was employed. A 25-dBi 0.652-THz source and the camera were placed at a far-field distance of 1 m. For rotational scanning, the camera was mounted onto a 6-axis table-top robot arm, and it was scanned over a $\pm 25° \times \pm 25°$-sector of the hemisphere to capture all pixel beams, with a lateral step size of 0.5°. A camera frame was acquired and stored in a 4-D measurement matrix at each scan position, out of which 2-D single-pixel far-field radiation patterns were extracted in data post-processing. Frame-averaging of 1024 frames aided to improve the integrated NEP from 583 nW to 18.2 nW at the source radiation frequency of 0.652 THz [3], [4]. Exemplarily, Fig. 2(a) and (b) show 1-D normalized single-pixel far-field radiation pattern cross-section cuts along θ and ϕ for pixels in a chip diagonal, respectively; the color bars indicate the normalized off-axis displacement (x/R), as the ratio of off-axis displacement to lens radius. In order to generate the desired beam incidence angle grid, the 2-D beam incidence angle coordinate was determined for each pixel by calculating the 2-D moment of associated single-pixel far-field radiation patterns. Values under –3 dB were set to zero, which is to say, only the main lobe was considered to determine the 2-D coordinate of the beam incidence angle. Fig. 3(a) shows the beam incidence angle grid generated, indicating barrel distortion. Exemplarily, in this figure, values associated with pixels that situate in a chip diagonal are correlated to their normalized off-axis displacement. In [5], [6], an equation is given to calculate the beam incidence angle (or scan angle), θ, based on simplified geometrical optics principles, namely $\theta = \tan^{-1}\left(\frac{x}{L}\right)$, with x and L being off-axis displacement and lens extension length, respectively. In Fig. 3(b), diagonal values along θ and ϕ, as marked in Fig. 3(a), are compared with calculated values using the given equation. From inspection of this figure, it is clear

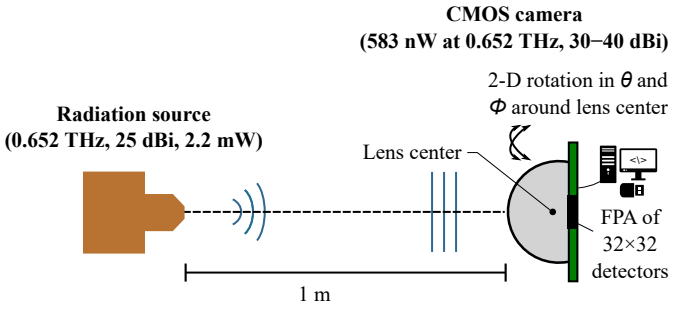

Figure 1. Experimental setup employed to measure single-pixel far-field radiation patterns of the silicon lens-integrated CMOS THz camera.

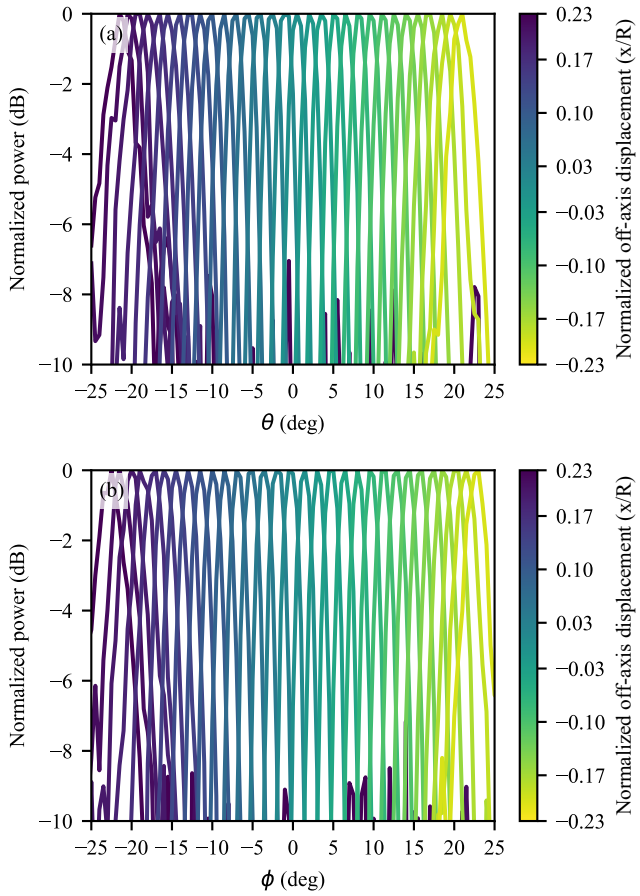

Figure 2. Normalized single-pixel radiation pattern cross-section cuts for pixels situated in a chip diagonal along θ (a) and ϕ (b).

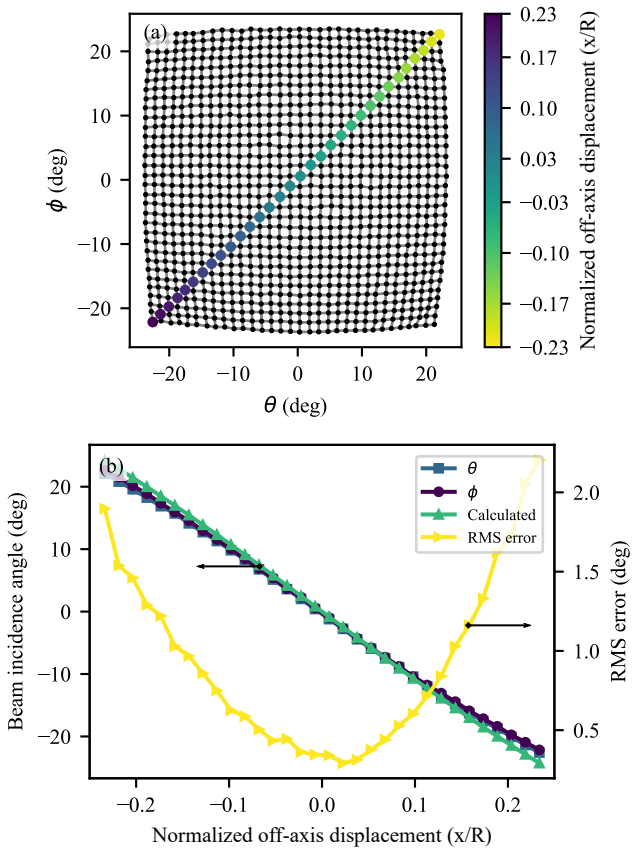

Figure 3. (a) Measured beam incidence angle grid, indicating barrel distortion; the colorbar describes the normalized off-axis displacement for marked pixels in the FPA diagonal. (b) Values along θ and ϕ for such pixels compared with calculated ones and the RMS error of calculated values based on measured ones, both plotted as a function of the normalized off-axis displacement.

that the equation is a good approximation for pixels placed in the very center, as the RMS error (right axis) is near zero. However, for larger normalized off-axis displacement or larger beam incidence angles, the RMS error accelerates in a quadratic manner. The particular problem with the equation is that it only considers the central ray. Thus, the beam incidence angle grid determined will enable better geometric camera calibration, which will be particularly valuable for light-field imaging [5], [7] and source characterization [8]–[12]. The findings are important for beam switching applications other than imaging, such as communications or radar, since the radial distortion directly relates to the intensively studied subject "scan angle".

Acknowledgment

The authors thank Ticwave GmbH, Wuppertal, Germany, for providing the CMOS THz camera. DFG funded this work through the individual grant project "Spatially-Mapped Mobile Terahertz Spectroscopy (T-MAP)".

References

[1] D. F. Filipovic, G. P. Gauthier, S. Raman, and G. M. Rebeiz, "Off-axis properties of silicon and quartz dielectric lens antennas," *IEEE Trans. Antennas Propag.*, vol. 45, no. 5, pp. 760–766, 1997.

[2] R. Al Hadi, H. Sherry, J. Grzyb, Y. Zhao, W. Forster, H. M. Keller, A. Cathelin, A. Kaiser, and U. R. Pfeiffer, "A 1 k-Pixel Video Camera for 0.7–1.1 Terahertz Imaging Applications in 65-nm CMOS," *IEEE J. Solid-State Circuits*, vol. 47, no. 12, pp. 2999–3012, 2012.

[3] R. Zatta, R. Jain, and U. R. Pfeiffer, "Characterization of the noise behavior in lens-integrated CMOS terahertz video cameras," *Terahertz Sci. Techn.—Int. J. THz*, vol. 11, no. 4, pp. 102–123, Dec. 2018.

[4] V. S. Jagtap, R. Zatta, J. Grzyb, and U. R. Pfeiffer, "Performance Characterization Method of Broadband Terahertz Video Cameras," in *Proc. Int. Conf. Infrared Millim. Terahertz Waves*, Sep. 2019.

[5] R. Jain, J. Grzyb, and U. R. Pfeiffer, "Terahertz Light-Field Imaging," *IEEE Trans. Terahertz Sci. Technol.*, vol. 6, no. 5, pp. 649–657, 2016.

[6] H. Frid, "Closed-Form Relation Between the Scan Angle and Feed Position for Extended Hemispherical Lenses Based on Ray Tracing," *Appl. Phys. Lett.*, vol. 15, pp. 1963–1966, 2016.

[7] R. Jain, P. Hillger, J. Grzyb, E. Ashna, V. Jagtap, R. Zatta, and U. R. Pfeiffer, "A 32×32 Pixel 0.46-to-0.75THz Light-Field Camera SoC in 0.13µm CMOS," in *Proc. IEEE Int. Solid-State Circuits Conf.*, vol. 64, Feb. 2021, pp. 484–486.

[8] D. Headland, R. Zatta, P. Hillger, and U. R. Pfeiffer, "Terahertz Spectroscope Using CMOS Camera and Dispersive Optics," *IEEE Trans. Terahertz Sci. Technol.*, pp. 513–523, 2020.

[9] D. Headland, P. Hillger, R. Zatta, and U. Pfeiffer, "Incoherent, spatially-mapped THz spectral analysis," in *Proc. Int. Conf. Infrared Millim. Terahertz Waves*, Sep. 2018.

[10] R. Zatta, V. S. Jagtap, J. Grzyb, and U. R. Pfeiffer, "CMOS THz Camera Used as Compact Antenna Test Range," in *Proc. Int. Worksh. Mob. Terahertz Syst.*, Jul. 2020.

[11] ——, "CMOS Camera-Type THz Compact Antenna Test Range for Far-Field Radiation Pattern Analysis," in *Proc. Int. Conf. Infrared Millim. Terahertz Waves*, Nov. 2020.

[12] V. S. Jagtap, R. Zatta, S. Nellen, B. Globisch, J. Grzyb, and U. R. Pfeiffer, "Broadband Spectro-Spatial Characterization of CW Terahertz Photoemitter Using CMOS Camera," in *Proc. Int. Conf. Infrared Millim. Terahertz Waves*, Nov. 2020.